Science and Technology Publishing (SCI & TECH)
ISSN: 2632-1017
Vol. 8 Issue 6, June - 2024

Analytical Modelling And Simulation Of Solid Waste Disposal Container Motion Parameters During Normal Trailer Mobility Condition

Eyo Akabom Joseph[1]
Department of Mechanical and Aerospace Engineering,
University of Uyo, Uyo, Akwaibom State-Nigeria

Aniekan Offiong[2]
Department of Mechanical and Aerospace Engineering,
University of Uyo, Uyo, Akwaibom State-Nigeria

Markson, I. E.[3]
Department of Mechanical Engineering
University of Uyo, Uyo Akwa Ibom State, Ngeria
idorenyinmarkson@uniuyo.edu.ng

Ozuomba Simeon[4]
Department of Electrical/Electronic and Computer Engineering
University of Uyo, Uyo Akwa Ibom State, Ngeria
simeonozuomba@uniuyo.edu.ng

Alexander Aniekan Offiong[5]
Department of Mechanical and Aerospace Engineering,
University of Uyo, Uyo, Akwaibom State-Nigeria

***Abstract*— The analytical modelling and simulation of solid waste disposal container motion parameters during normal trailer mobility condition is presented. The analytical models for the weight of the container, the velocity, acceleration, airspeed, drag force, drag moments, and slip angle of the vehicle as it transports the waste container to the destination of the waste are presented. The analytical models are essential for monitoring the incidences of tempering of the waste while on transit. The parameters are modelled in simulink and the simulations are conducted based on a given case study parameter specifications. The simulation results showed that the acceleration on the x-axis increased and normalized at 10km/hr2 within 0.083 hours (which is 4.98 minutes). The acceleration of the vehicle in y-direction normalized after 0.2 hrs (which is 12 minutes), The acceleration of the vehicle in y-direction failed to normalize as fast as that of the x-direction due to the force on the vehicle being more in y-direction. The drag moments on the vehicle increased normally and became saturated after 0.2 hours. The load of the waste in the container was 10 tonnes. The detailed simulation results showed that the models can be used to effectively monitor the key motion parameters of the waste container and its weight while the vehicle is in normal motion condition. This will help in the design of tampering monitoring mechanism which will checkmate unauthorized removal of toxic waste during the waste disposal.**

***Keywords*— Solid Waste, Tampering Monitoring Mechanism, Waste Disposal, Airspeed, Drag Force, Drag Moments, Slip Angle**

1. INTRODUCTION

Nowadays, the use of emerging Internet of Things (IoT) is widely spreading across the globe [1, 2]. The use of IoT in the waste disposal management system is therefore part of the ongoing transition to smart systems technology [3, 4]. With such technology, it is possible to efficiently manage waste disposal in such a way that the waste bins are remotely monitored and only evacuated when the remote monitoring system indicates that the waste bin is full. Such technology will therefore minimize the time and other

resources used in the management of the waste evacuation from the waste bins [5,6].

Also, satellite mapping system can be used along with the population data to determine the appropriate locations for the waste bins and the capacity or number of a given waste in that can be located at any given site [7,8,9,10]. Historical data of the waste disposal system can be used to further optimize the waste disposal system [11,12,13]. Given the numerous possibilities that are afforded by the emerging technologies, in this paper, the focus is to still move the frontiers of possibilities by including tracking of waste on transit, with emphasis on identifying tampering incidence while the waste is on transit. This is particularly useful in monitoring toxic waste to avoid it being circulated in the society thereby endangering the life of members of the community [14,15]. Specifically, the paper presented mathematical model for capturing the dynamics of the weight, velocity and other forces on the waste disposal container under normal motion condition. The model serves as the basis for studying the effect of obstruction, tampering, and other factors on the weight, velocity and other forces on the waste disposal container. The models are then simulated using some sample dataset and the results are presented ad discussed.

2. METHODOLOGY

The solid waste is transported in a container by a trailer with requisite velocity and weight sensors, as well as communication circuitry that transmits the sensor data to remote server for personnel in charge of the waste disposal management system to assess the data and take actions appropriately. The focus in this study is to present the analytical model for the velocity and weight of the toxic solid waste container during normal trailer mobility condition. Based on the analytical models, the simulation is carried out using Matlab/Simulink software.

2.1 The analytical models of the solid waste container during the normal trailer mobility condition

For the dynamics, the acceleration A of the vehicle along x-axis is;

$$A_X = V_x r + \frac{F_{xfl}+F_{xrl}+F_{xext}}{M} \quad (1)$$

The acceleration for the y-axis is;

$$A_y = V_y r + \frac{(F_{yfl}+F_{yrl}+F_{yext})}{M} \quad (2)$$

The vehicle resultant velocity is;

$$V_r = \frac{\left(a(F_{xfl}+F_{yfl})-b(F_{xrl}-F_{yrl})+\frac{c(F_{xfl}-F_{yfl})}{2}+\frac{d(F_{xrl}-F_{yrl})}{2}\right)}{I_{zzz}} \quad (3)$$

Where A_x is the acceleration at the x-coordinates, A_y represents the acceleration at y-coordinates, V_r represents the resultant velocity of the toxic waste container, V_x represents the velocity at of the trailer at x-coordinates, V_y represents the velocity at y-coordinates. F_{xfl} , F_{yfl} represents the lateral force applied to the toxic load during the movement of the container in x and y coordinates respectively, F_{xrl} , F_{yrl} represents the lateral force applied to the left side and right side of the container during mobility of the trailer in x and y coordinates respectively, F_{xext} , F_{yext} represents the external force on x and y coordinates of the container during mobility and I_{zzz} represents the load inertia during transportation and a,b,c,d represents the distances of rear, front left side and right side wheel from the normal point of projection of the vehicle.

The airspeed is given;

$$ww_x = \sqrt{(V_x - W_{sx})^2 + (V_x + W_{sx})^2 + V_x^2 + W_{sx}^2} \quad (4)$$

$$ww_y = \sqrt{\left(V_y - W_{sy}\right)^2 + \left(V_y + W_{sy}\right)^2 + V_y^2 + W_{sy}^2} \quad (5)$$

$$ww_R = \frac{\left(\sqrt{V_r*\left((ww_x-ww_y)^2+(ww_x+ww_y)^2\right)}\right)}{ww_x^2+ww_y^2} \quad (6)$$

Where ww_x, ww_y and ww_R represents the airspeed of the container during mobility at x-coordinates, y-coordinates and resultant condition, W_{sx} and W_{sy} represents the wind speed at x and y coordinates and V_x, V_y and V_R represents the velocity of the container in x and y coordinates and the resultant velocity. The effect of the toxic load on the trailer mobility (drag moments) is given as;

$$f_{dx} = \frac{1}{2.5RT} A_{dx} a_f (ww_x)^2 \quad (7)$$

$$f_{dy} = \frac{1}{2.5RT} A_{dy} a_f \left(ww_y\right)^2 \quad (8)$$

$$f_{dR} = \sqrt{\frac{\left((f_{dx})^2-(f_{dy})^2\right)}{2f_{dx}f_{dy}}} \quad (9)$$

Where f_{dx}, f_{dy} and f_{dR} represents the drag force of the trailer vehicle on the toxic load in x and y coordinates and the resultant respectively, A_{dx} and A_{dy} represents the air drag coefficients the toxic load exerts on the mobile vehicle, a_f represents the front area of the mobile vehicle and ww_x, ww_y represents the airspeed of the container during mobility at x-coordinates, y-coordinates and R and T represents the atmospheric specific air constant and environmental air temperature respectively.

Hence, the drag moments are given as;

$$m_{dx} = \frac{f_{dx}}{1.4RT} c_{px} a_f P_a (a+b)^2 \quad (10)$$

$$m_{dy} = \frac{f_{dy}}{1.4RT} c_{py} a_f P_a (c+d)^2 \quad (11)$$

$$m_{dR} = \left(\sqrt{m_{dx}^2 + \frac{m_{dy}^2}{f_{dR}+ww_R}}\right. \quad (12)$$

Where m_{dx}, m_{dy} and m_{dR} represents the toxic waste container drag moments in x and y coordinates, and resultant respectively. The expected slip angles of the vehicle are;

$$Aft_x = \arctan\left(\frac{A_x+f_{dx}}{V_x-\left(\frac{m_{dx}}{m_{dR}}\right)}\right) \quad (13)$$

$$Aft_y = \arctan\left(\frac{A_y+f_{dy}}{V_y-\left(\frac{m_{dy}}{m_{dR}}\right)}\right) \quad (14)$$

$$Aft_R = \left(\left(\frac{1}{Aft_x}\right)^{0.5} + \left(\frac{1}{Aft_y}\right)^{0.5}\right) m_{dR} \quad (15)$$

Where Aft_x, Aft_y and Aft_R represents the slip angles of the wheels of the vehicle at x and y coordinates and resultant, A_x and A_y are the dynamic acceleration of the vehicle in x and y coordinates, V_x and V_y represents the dynamic velocity of the vehicle and m_{dR} represents the resultant drag moments of the container.

The expected or normal velocity of the vehicle (which would be the same for all the sensor positions) from kick off of the vehicle to the normalized velocity is given as;

$$V_n = \left(\frac{\sqrt{A_x^2 + A_y^2}}{t}\right) - \frac{V_R - f_{dR}^{\frac{3}{2}}}{1.6RT} + \frac{m_{dR}}{Aft_R} \quad (16)$$

Where V_n is the normal velocity of the vehicle and t represents the time.

The weight of the container at normal speed (the container would be uniform at all the sensor points) determined and also the total force exerted on the container during motion of the vehicle is given as;

$$F_x = \frac{f_{dx}}{RT} \times \frac{ww_x}{Aft_x} A_x \quad (17)$$

$$F_y = \frac{f_{dy}}{RT} \times \frac{ww_y}{Aft_y} A_y \quad (18)$$

$$F_R = \sqrt{(F_x)^2 + \left(F_y\right)^2} \quad (19)$$

The weight of the container at normal condition is given as;

$$W_n = \frac{(F_R \times V_n)}{t} + \frac{m_{dR}}{2} \quad (20)$$

Where W_n represents the weight of the toxic waste container during motion at normal condition, V_n represents the speed of the Vehicle and F_x, F_y and F_R represents the total forces exerted on the container in x and y coordinates and the resultant.

The weight of the container during acceleration is given as;

$$W_{acc} = (F_R^{1.3} \times W_n) \times \frac{Log(W_n)}{V_n \times t} \quad (21)$$

Where W_{acc} represents the weight of the container during acceleration at normal condition.

The weight of the container during deceleration is given as;

$$W_{deccn} = W_n + \left(\frac{F_R^{1,3}}{V_n + t}\right) \quad (22)$$

Where W_{deccn} represents the weight of the container during deceleration at normal condition.

The weight of the container at zero acceleration (at uniform velocity) is the same as the weight of the container obtainer at velocity V_n. The flow chart for the pattern of the modeling is shown in Figure 1.

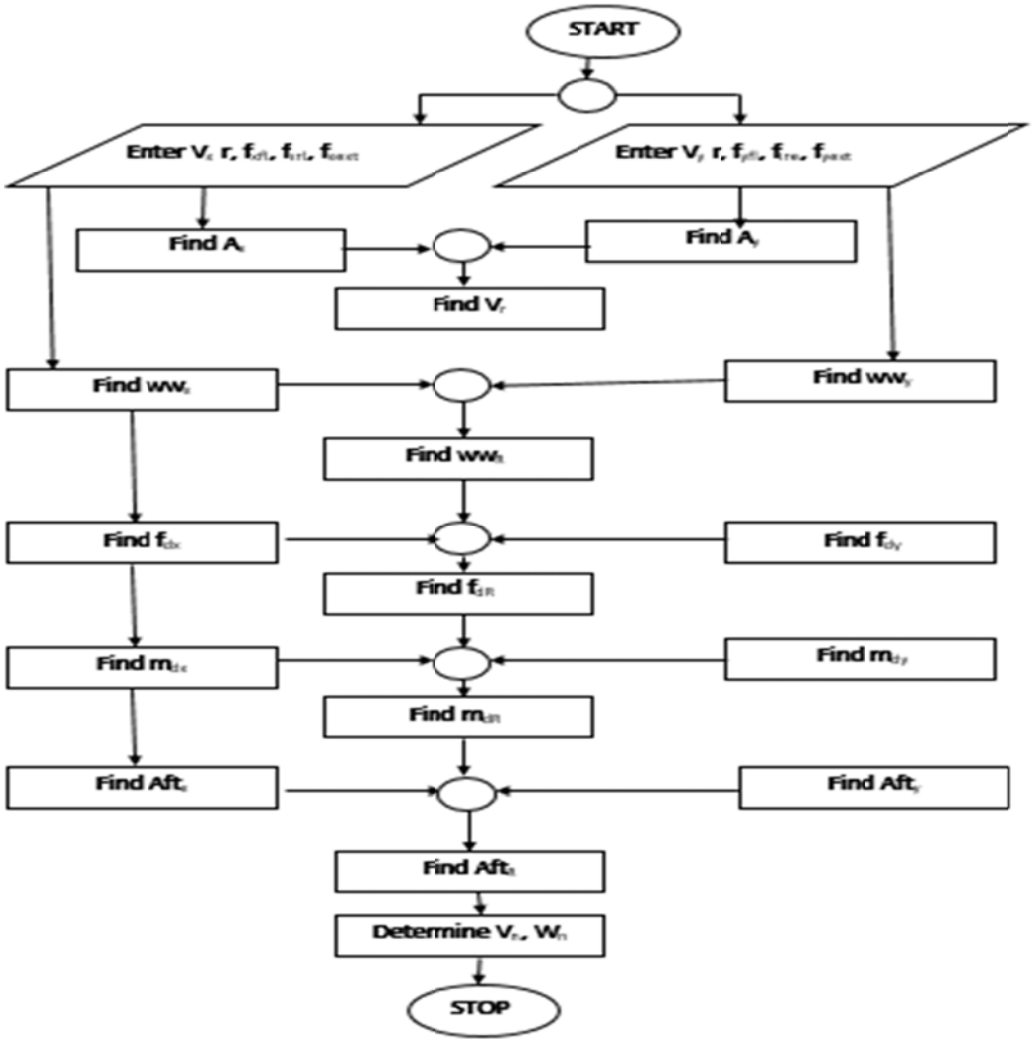

Figure 1; Flow diagram of velocity and Weights of toxic waste at normal condition

2.2 Simulink model of the solid waste container during the normal trailer mobility condition

The simulink model for the acceleration in x-coordinate as shown in Equation 1 is shown in Figure 2. The simulink model for the velocity at y-coordinate as displayed in Equation 2 is shown in Figure 3. The resultant velocity as shown in Equation 3 was displayed in Figure 4. The airspeed mobility for x and y coordinates as shown in Equation 4 and Equation 5 are displayed in Figure 5 and Figure 6 respectively. The resultant airspeed as shown in Equation 6 is shown in Figure 7. The simulink model for the drag moment force as shown in Equation 7, Equation 8 and Equation 7 for x-coordinates, y-coordinates and the resultant drag moments are displayed in Figure 8, Figure 9 and Figure 10 respectively.

The simulink model for the actual drag moment as shown in Equation 10, Equation 11 and Equation 10 for x-coordinates, y-coordinates and the resultant drag moments are displayed in Figure 11, Figure 12 and Figure 13 respectively. The simulink model for the slip angle of the wheel as shown in Equation 13, Equation 14 and Equation 15 for x-coordinates, y-coordinates and the resultant drag moments are displayed in Figure 12, Figure 15 and Figure 16 respectively.

The simulink model for the velocity in Equation 17 of the trailer is shown in Figure 17. The simulink model of the total force exerted on the container during motion for x and y coordinates and resultant as shown in Equation s 18, Equation 19 and Equation 20 are displayed in Figure 18, Figure 19 and Figure 20 respectively. Therefore, the simulink model of the weight of the load during motion of the truck as shown in Equation 21 is displayed in Figure 21.

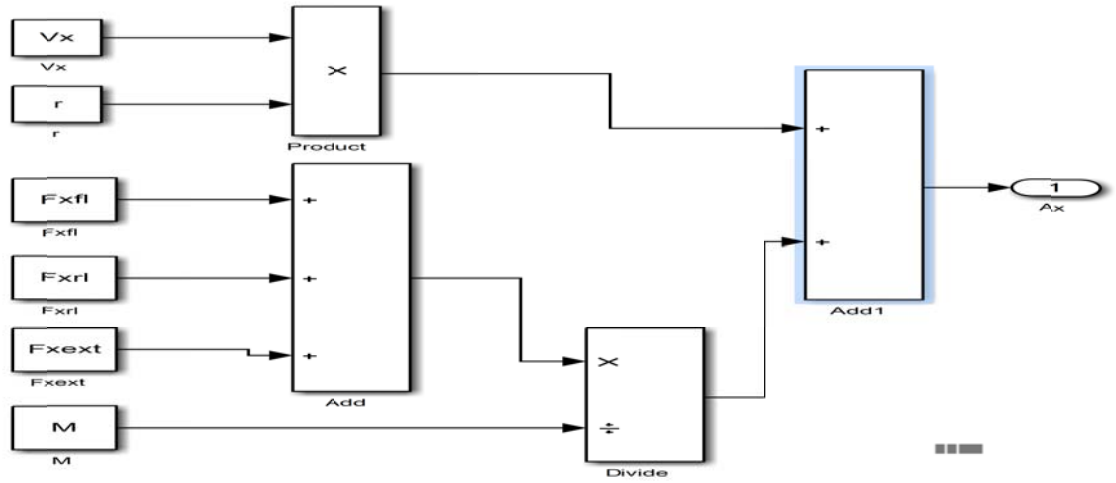

Figure 2; Simulink model for the Acceleration at x-coordinate

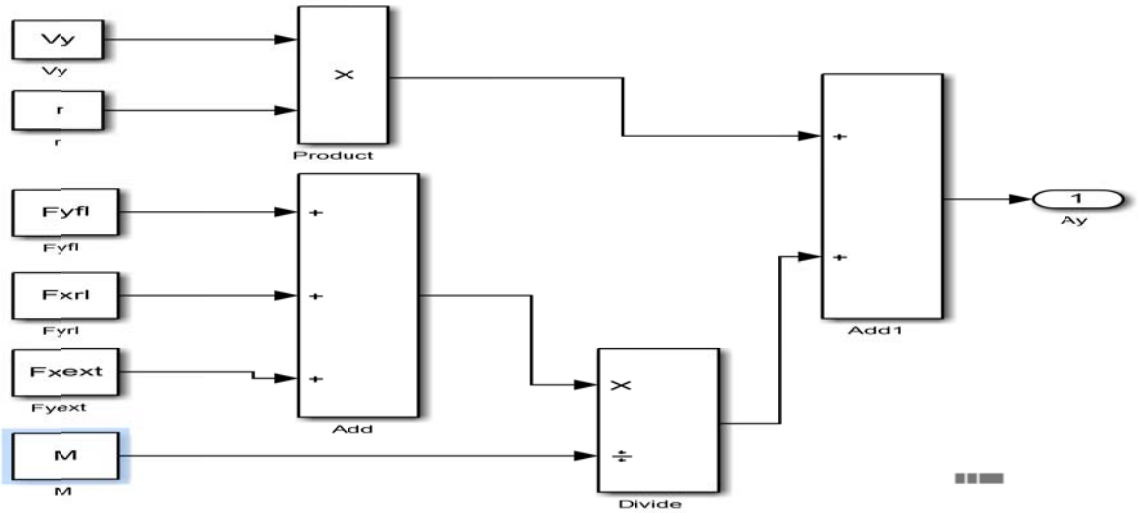

Figure 3; Simulink model for velocity at y-coordinate

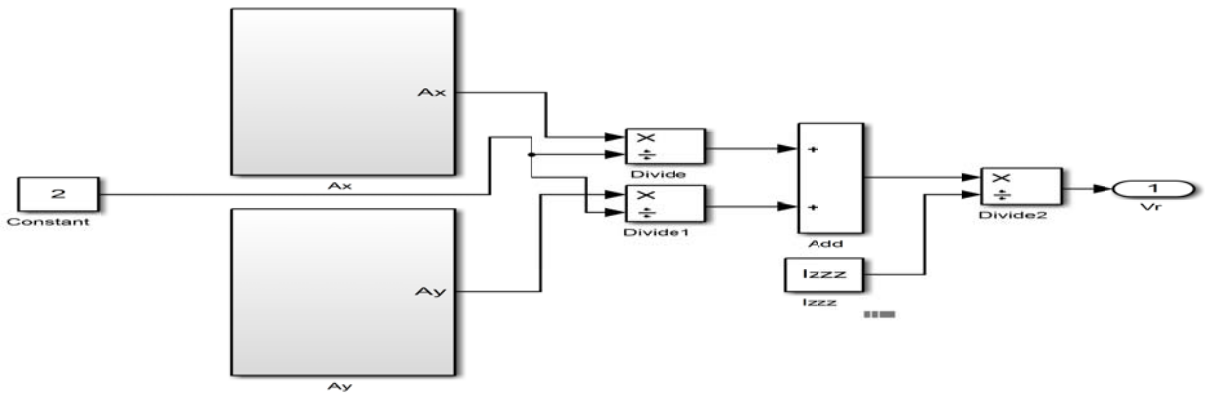

Figure 4. The resultant velocity

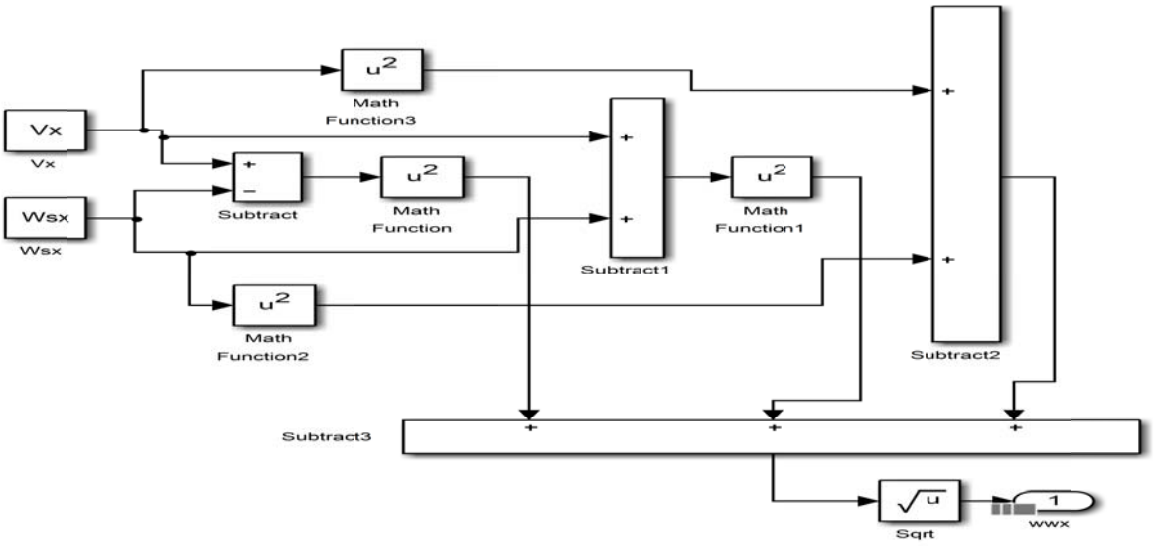

Figure 5; Airspeed mobility for x-coordinates

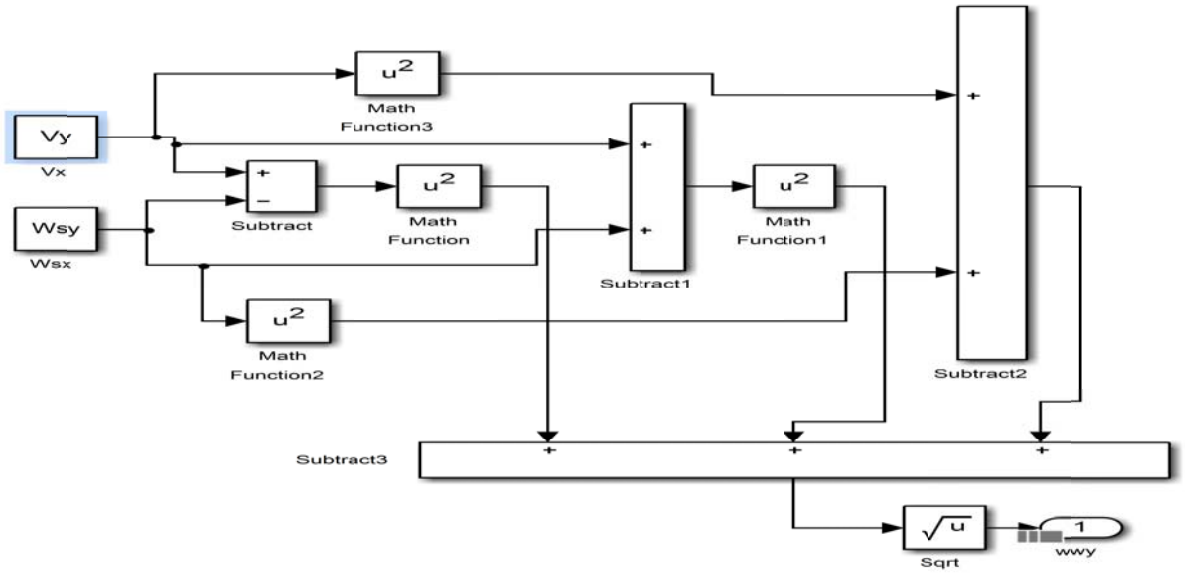

Figure 6; Airspeed mobility for y-coordinates

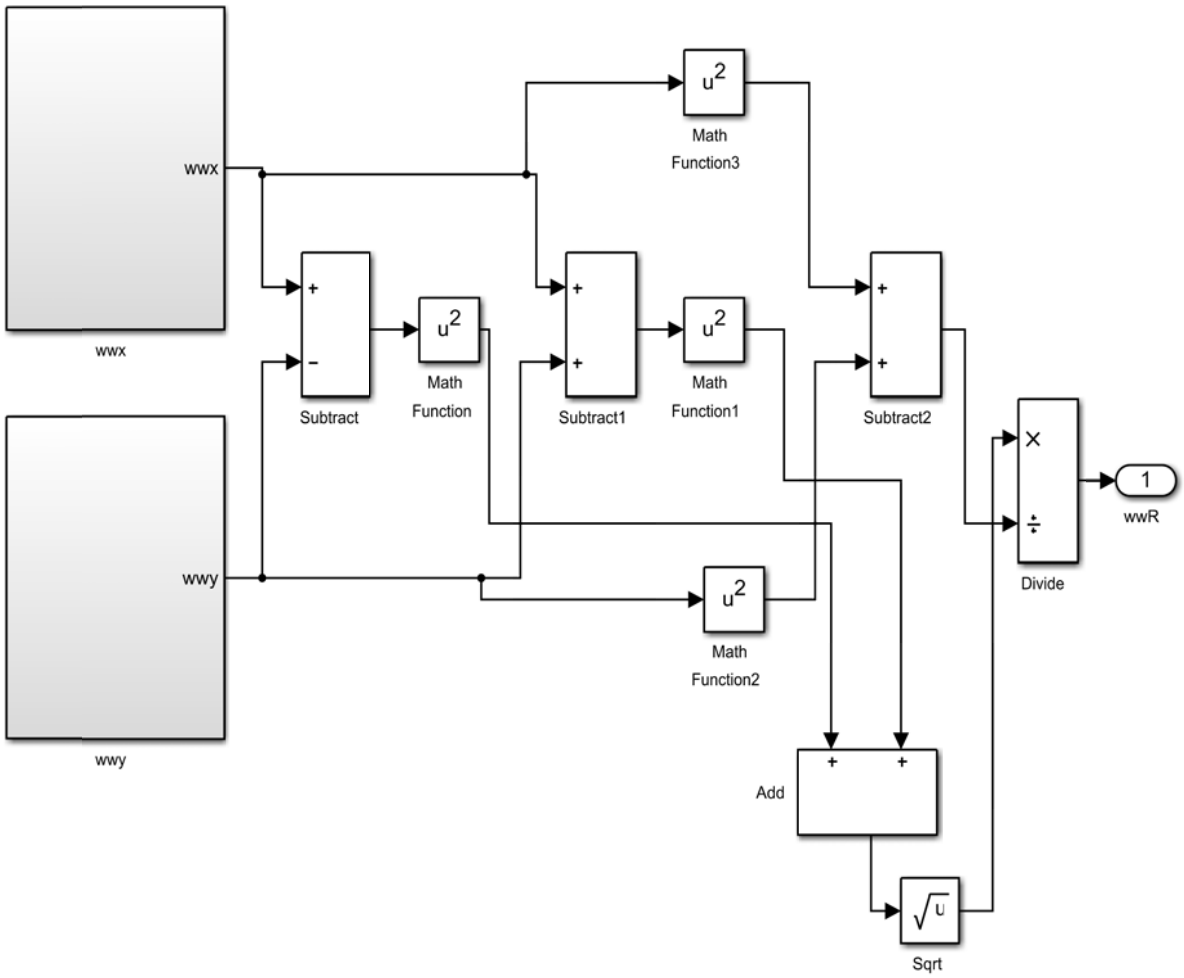

Figure 7; Resultant Airspeed

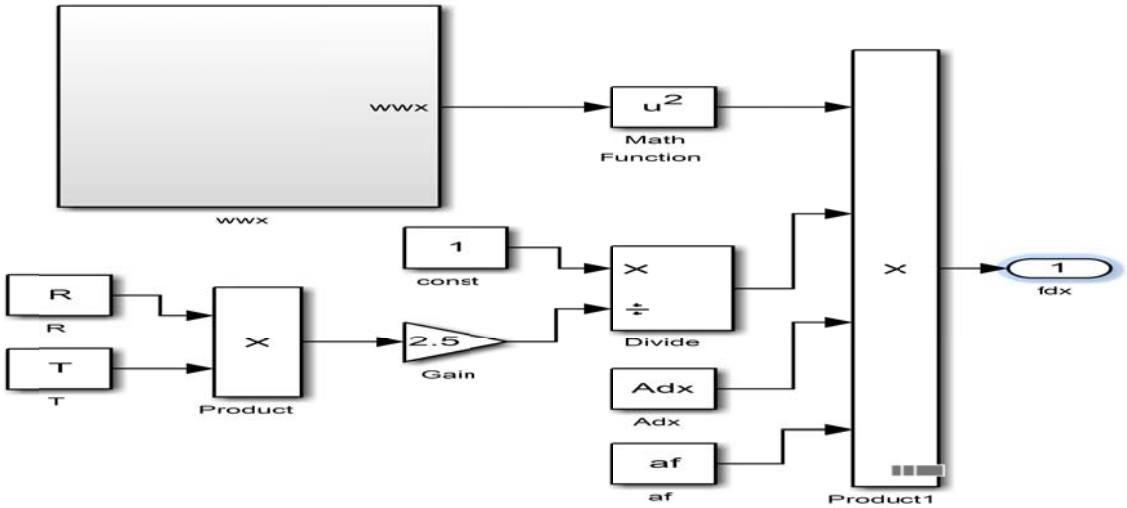

Figure 8; x-coordinates of the drag moments force

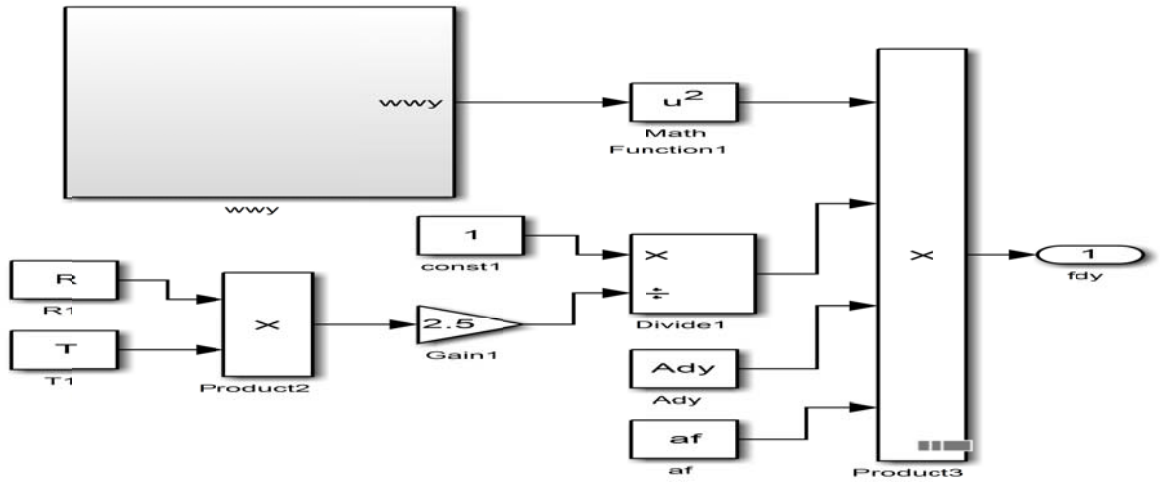

Figure 9; y-coordinates of the drag moments force

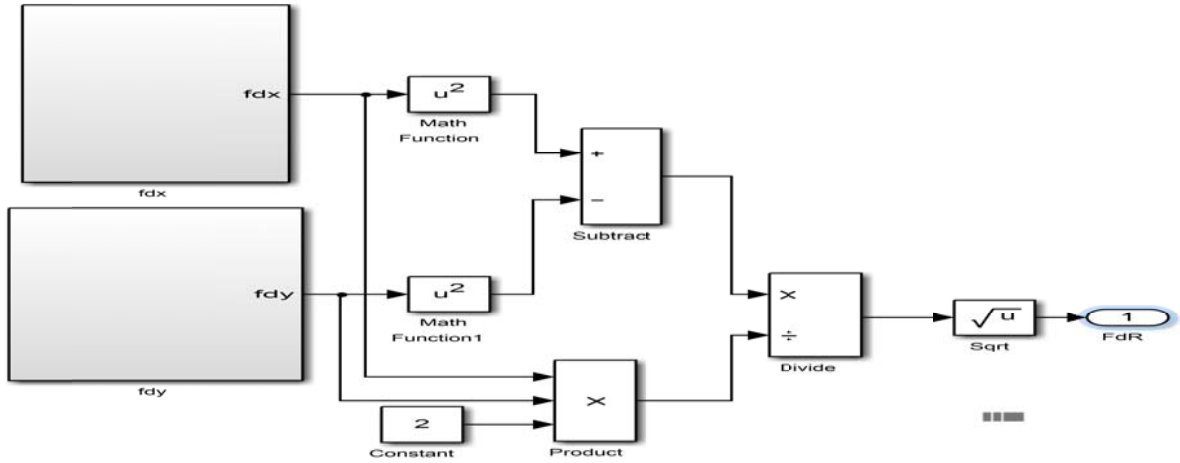

Figure 10; Resultant of the drag moment force

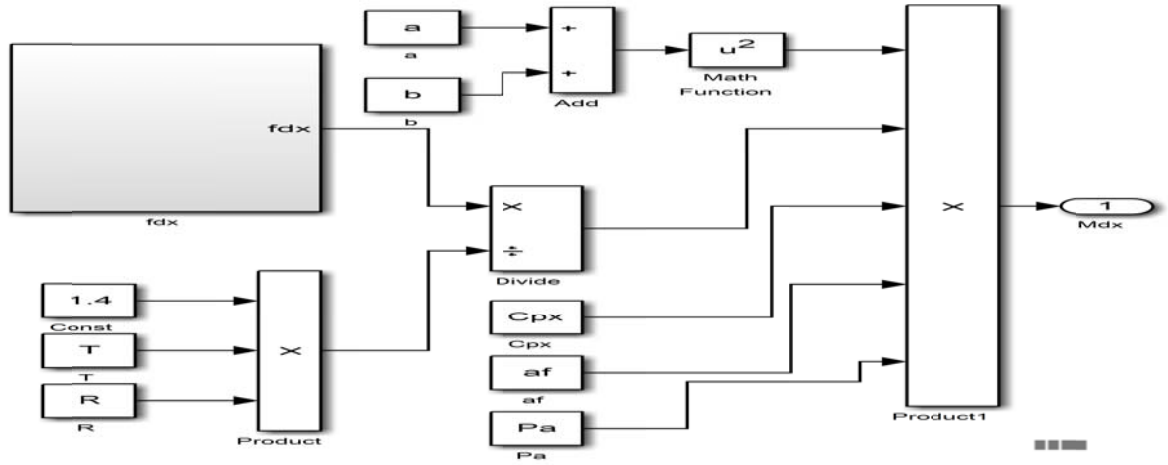

Figure 11; Actual moments in x-direction

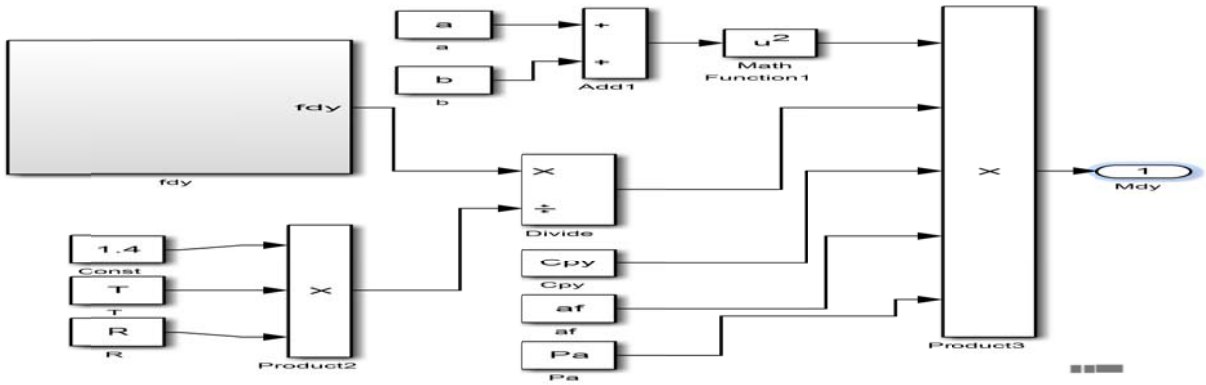

Figure 12; Actual moments in y-coordinates

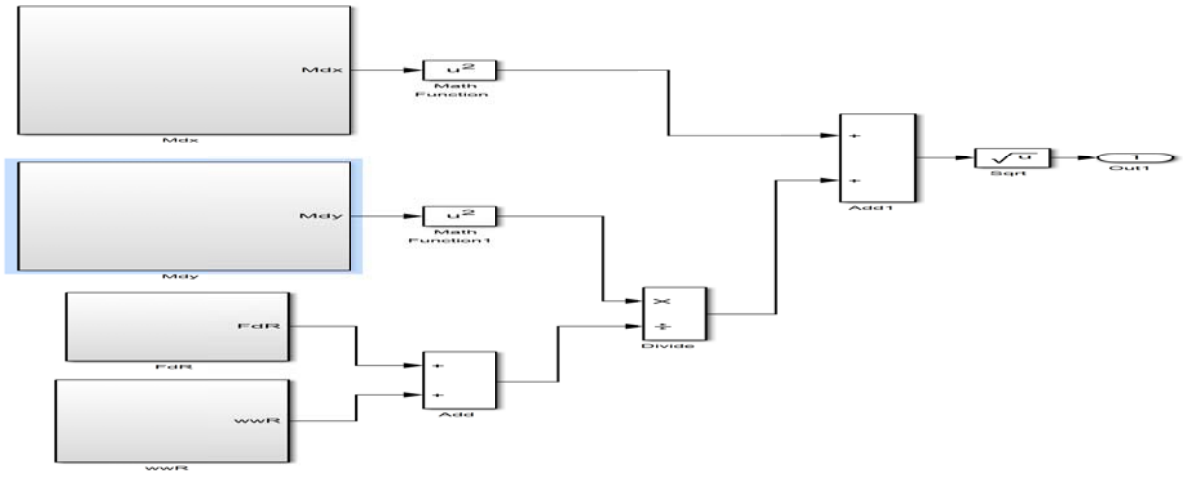

Figure 13; Resultant actual moments

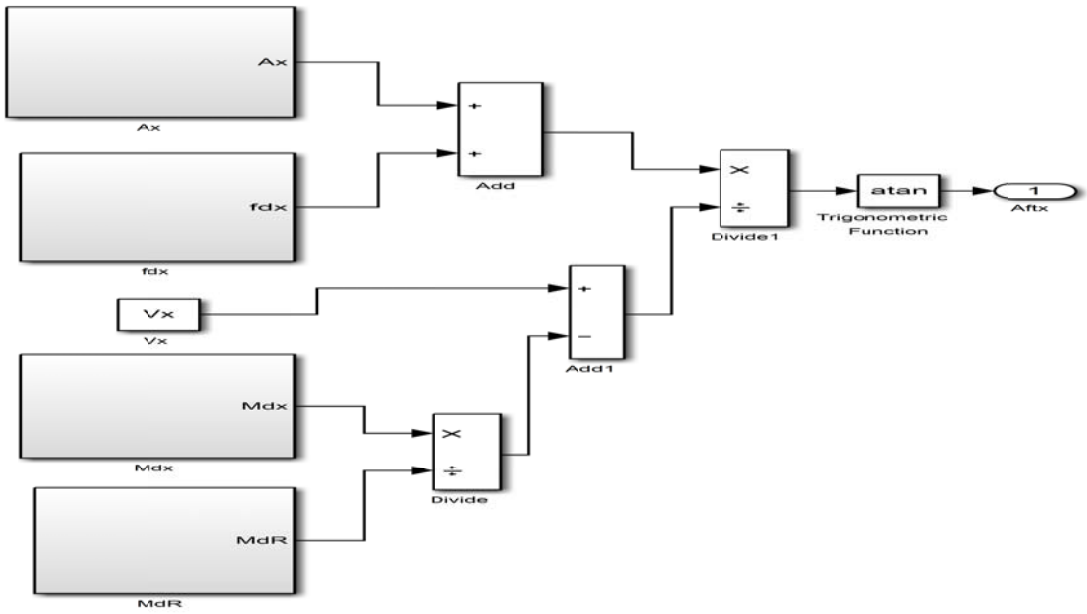

Figure 14; Slip angle of the wheel at x-direction

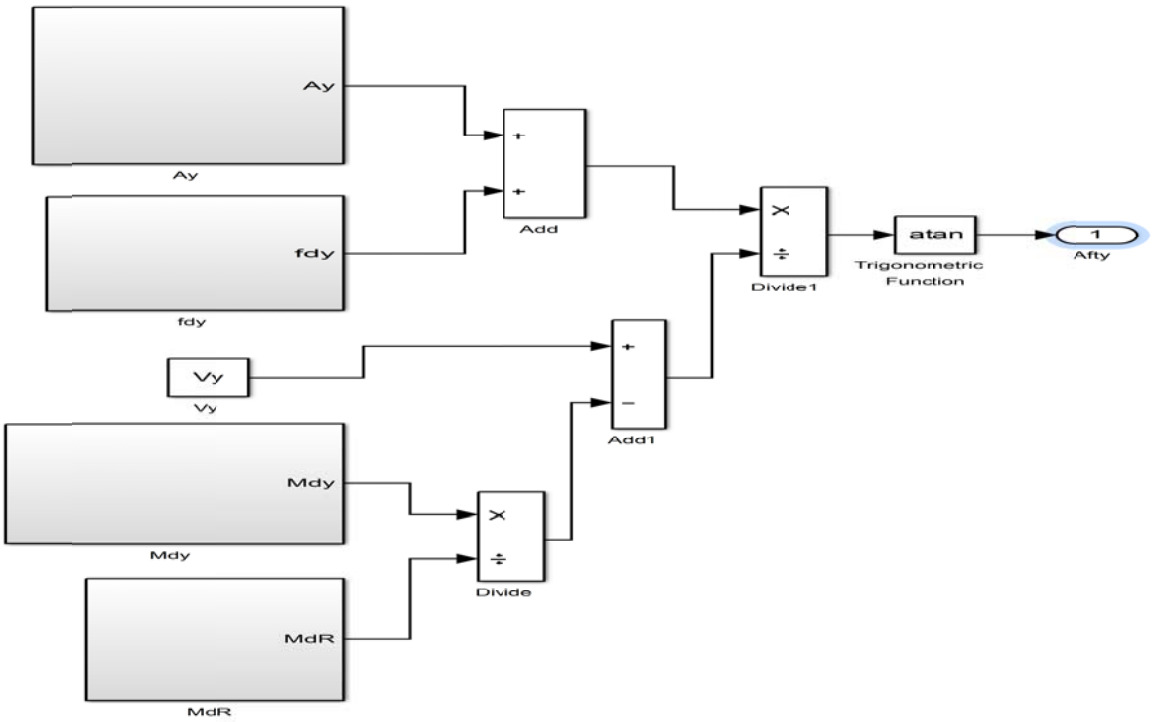

Figure 15; Slip angle of the wheel at y-direction

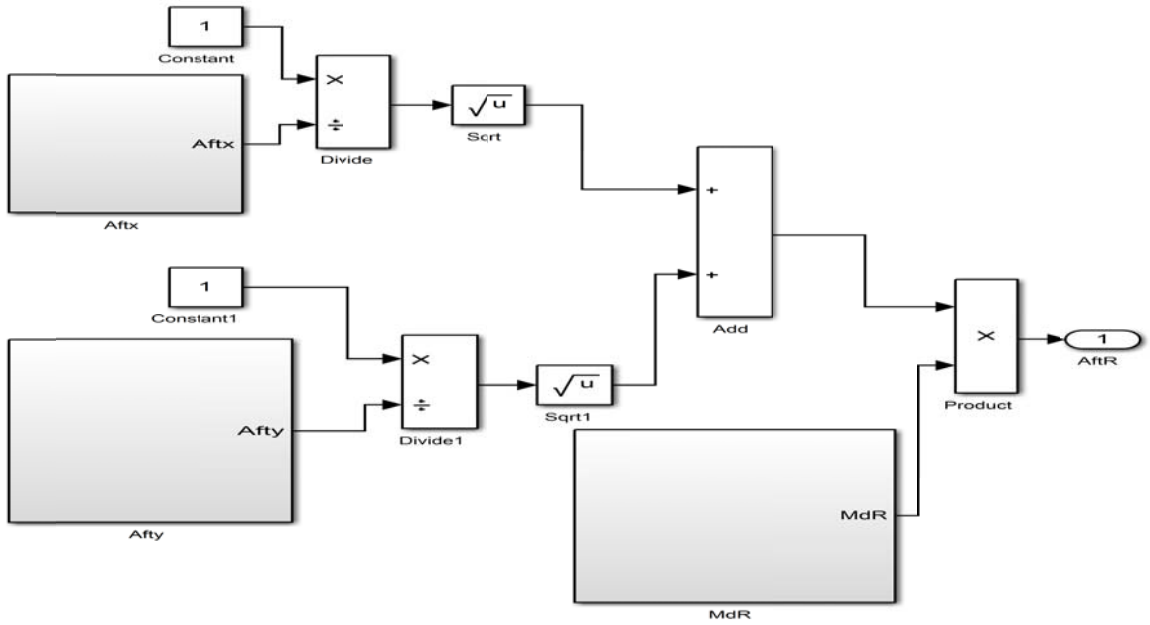

Figure 16; Resultant split angle of the wheel

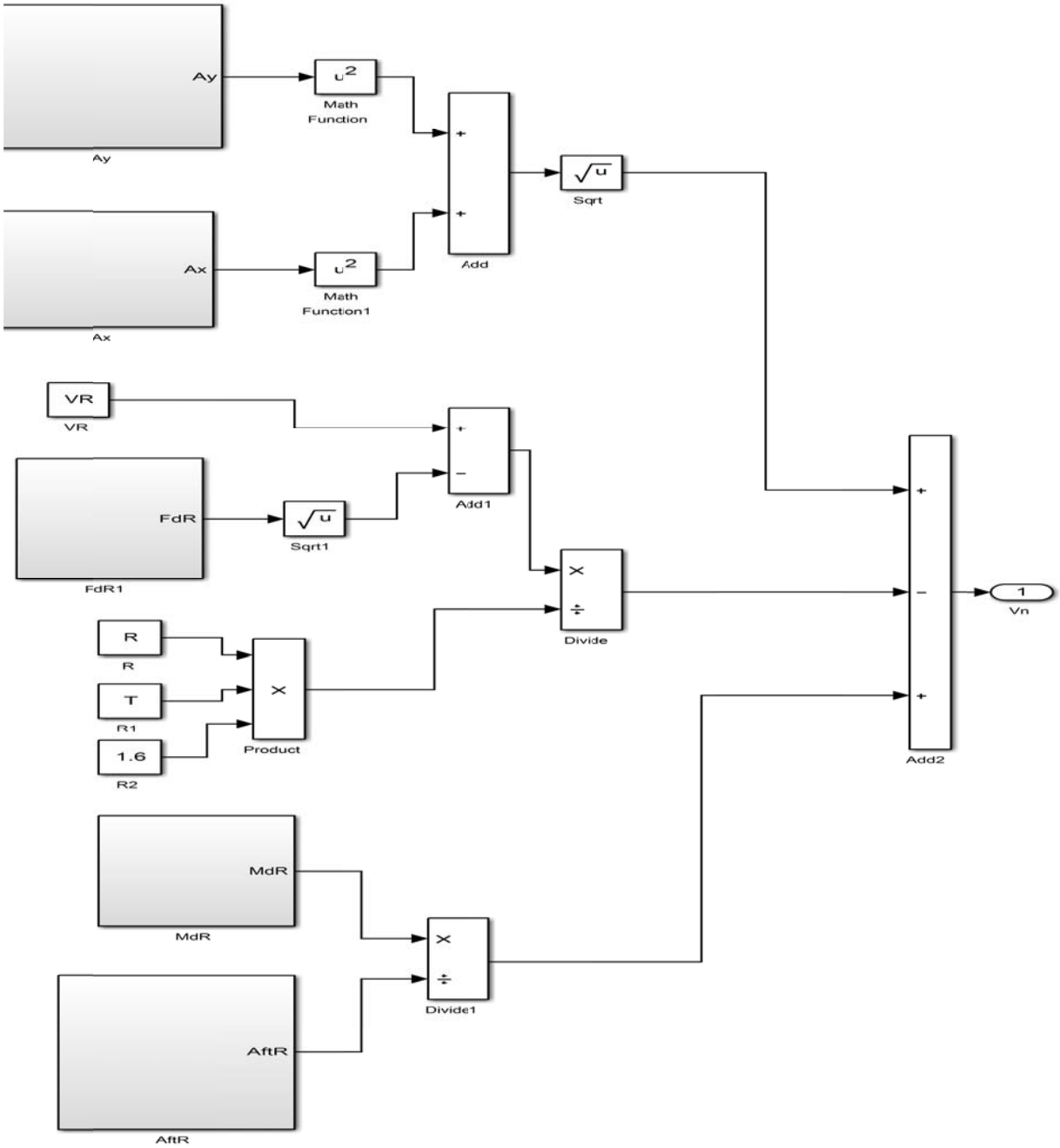

Figure 17; Normal velocity of the vehicle

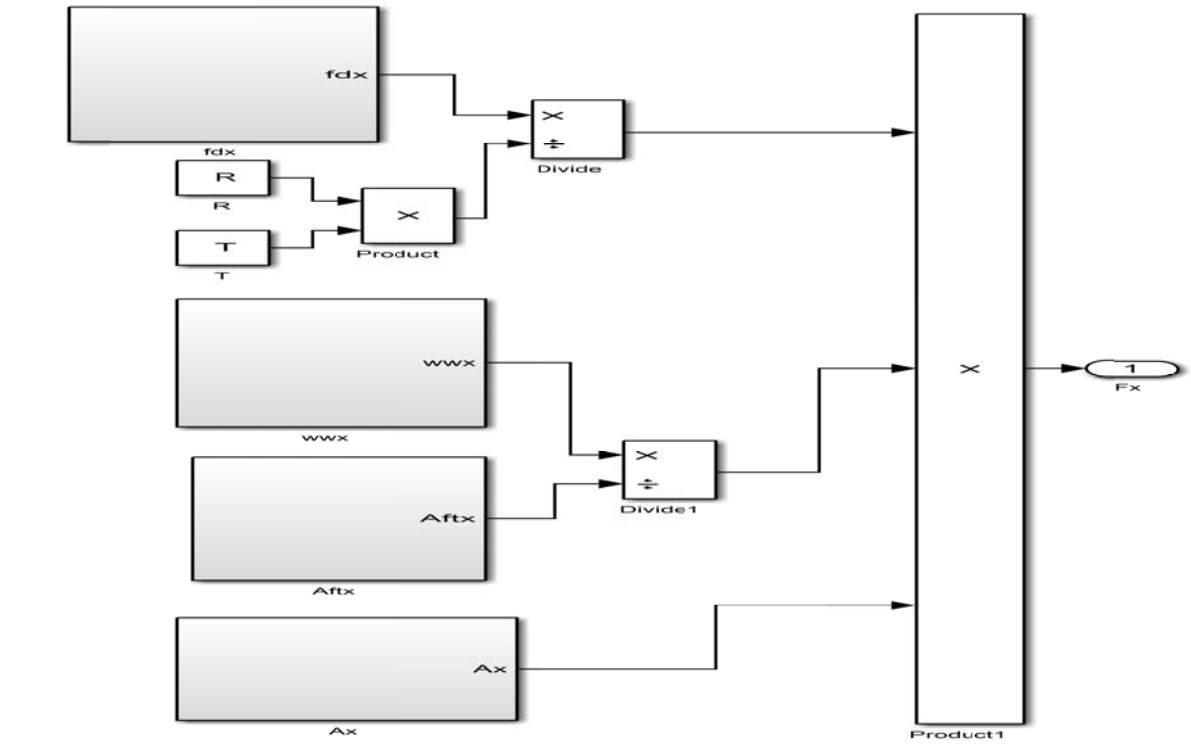

Figure 18; Force exerted on the load at x-direction

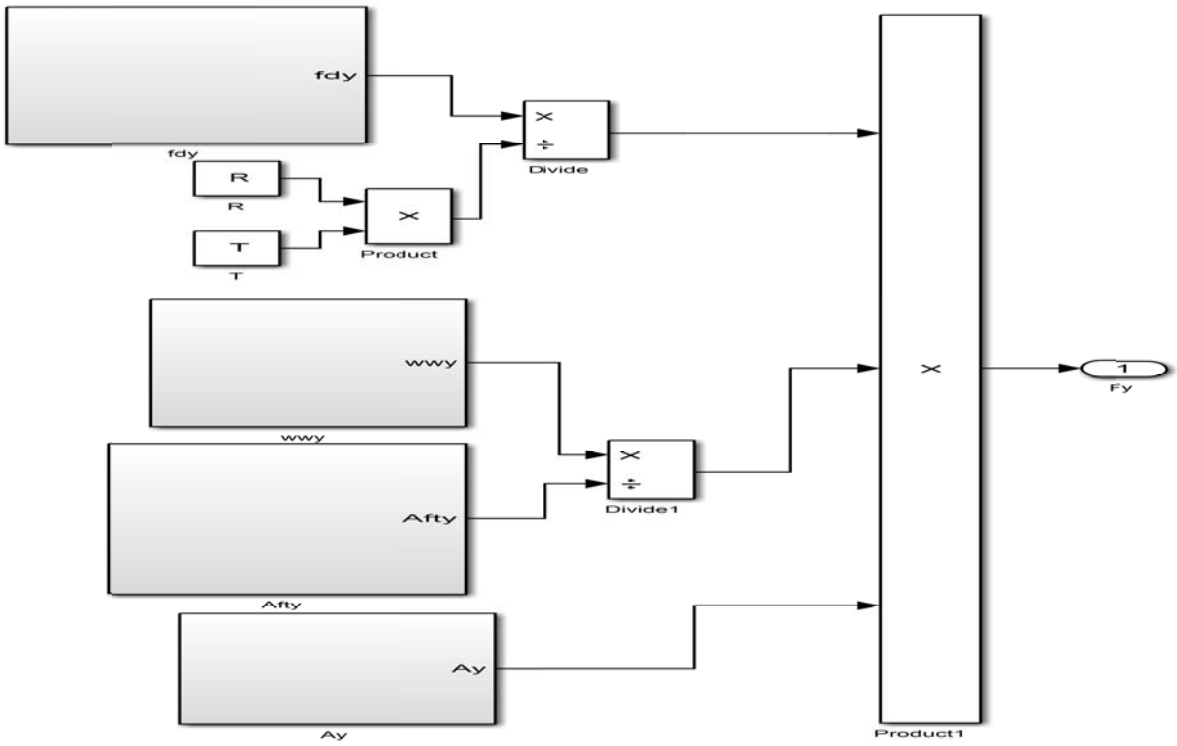

Figure 19; Force exerted on the load at y-direction

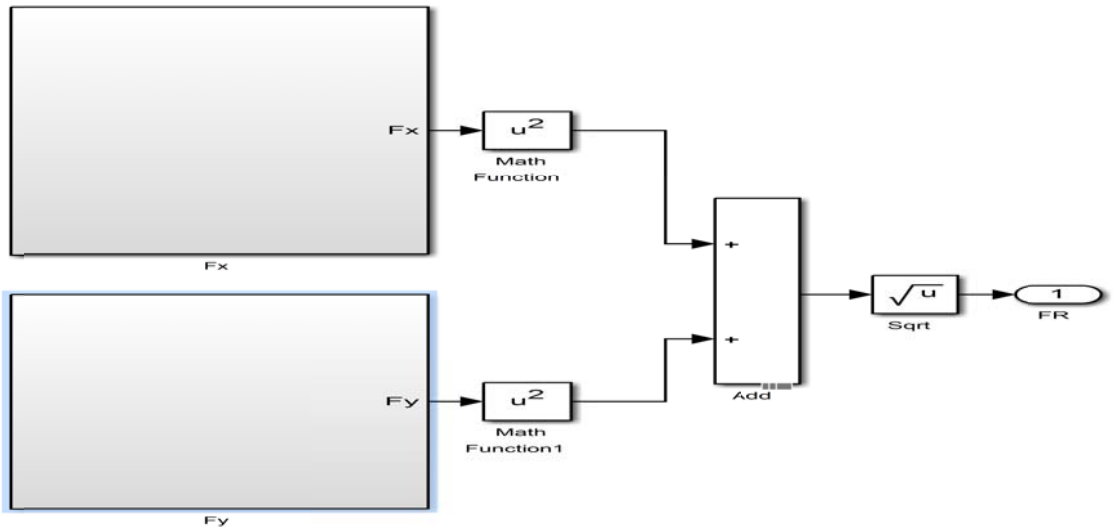

Figure 20; Resultant Force exerted on the load

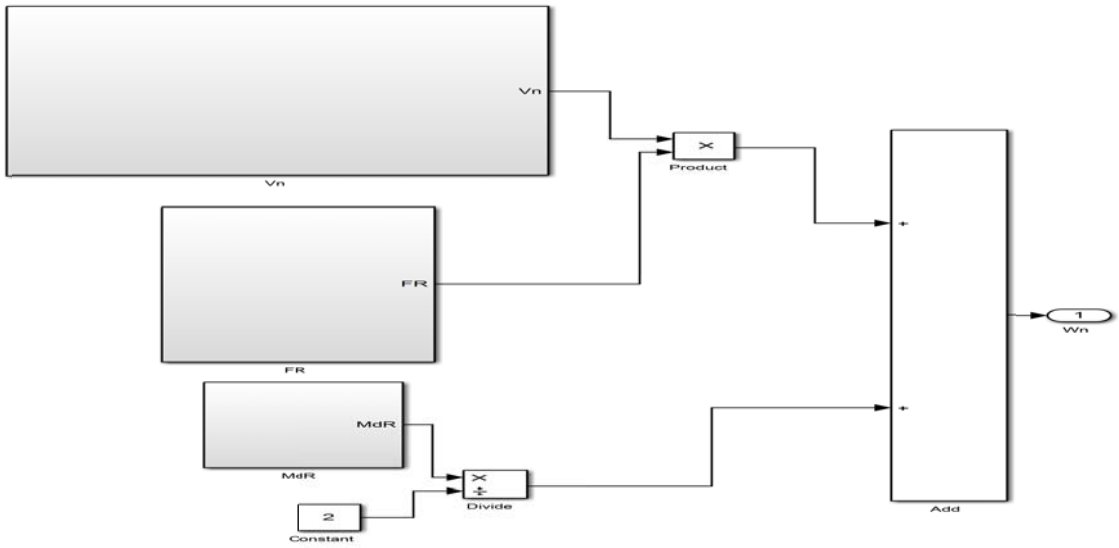

Figure 21; Simulink model of the weight of the container at normal motion

3. RESULTS AND DISCUSSION

Based on the waste container dimensions and the analytical models developed, the entire system after being modeled in Simulink environment was then simulated and results obtained are presented in this section.

3.1 Results on the acceleration of the vehicle in x-direction:

The plot for the acceleration of the vehicle with toxic waste as captured by the sensors is shown in Figure 22. The plot in Figure 22 showed that the acceleration on the x-axis increased and normalized at 10km/hr^2 within 0.083 hours (which is 4.98 minutes). The point was described as the normalized acceleration of the vehicle in the x-axis which was transmitted by the sensors to the remote server.

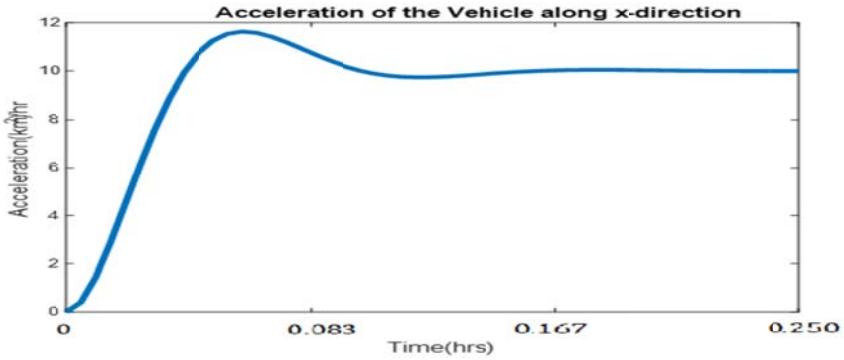

Figure 22; Acceleration of the vehicle along x-direction

3.2 Results on the acceleration of the vehicle in y-direction:

The acceleration of the vehicle in y-direction is shown in Figure 23. The plot in Figure 23 showed that the acceleration on the y-axis increased and started normalizing at 10km/hr^2 within 0.091 hours (which is 5.46 minutes). The point was described as the normalized acceleration of the vehicle in the y-axis which was transmitted by the sensors to the remote server.

It was observed in Figure 23 that the acceleration of the vehicle in y-direction failed to normalize as fast as that of the x-direction but was normalized at 10km/hr^2. This was due to the force on the vehicle being more in y-direction of the moving vehicle. This instability affected the speed of the vehicle which means that the weight of the toxic waste was excessive for the truck. However, the acceleration was normalized after 0.2 hrs (which is 12 minutes).

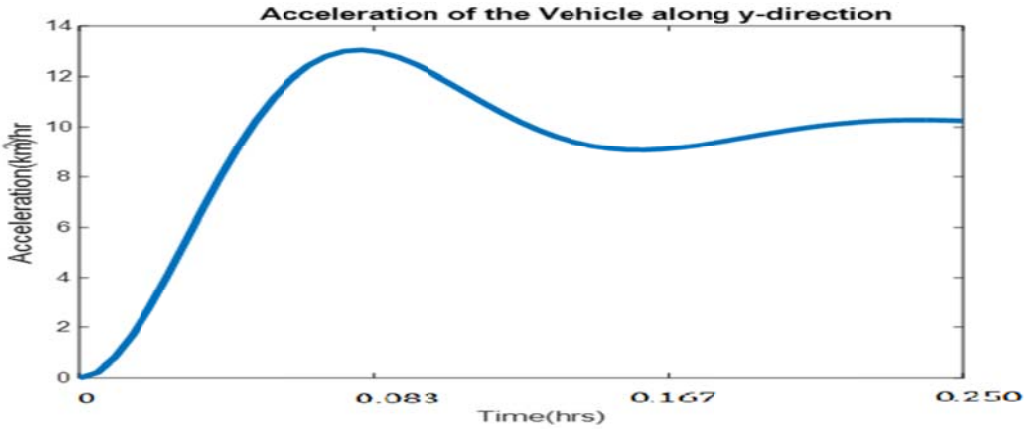

Figure 23; Acceleration of the Vehicle at y-direction

3.3 Results on the resultant velocity:

From the x-y directional acceleration, the resultant velocity of the vehicle is shown in Figure 24. The resultant velocity as shown in Figure 24 was initially unstable as shown but normalized and increased linearly after 0.2 hrs (which is 12 minutes) of motion. This was as the result of the anomaly with the acceleration at the y-direction as a result of the toxic waste load. The velocity in Figure 24 is the velocity obtained from the resultant acceleration of Figure 22 and Figure 23 and this velocity is transmitted by the sensors to the remote server.

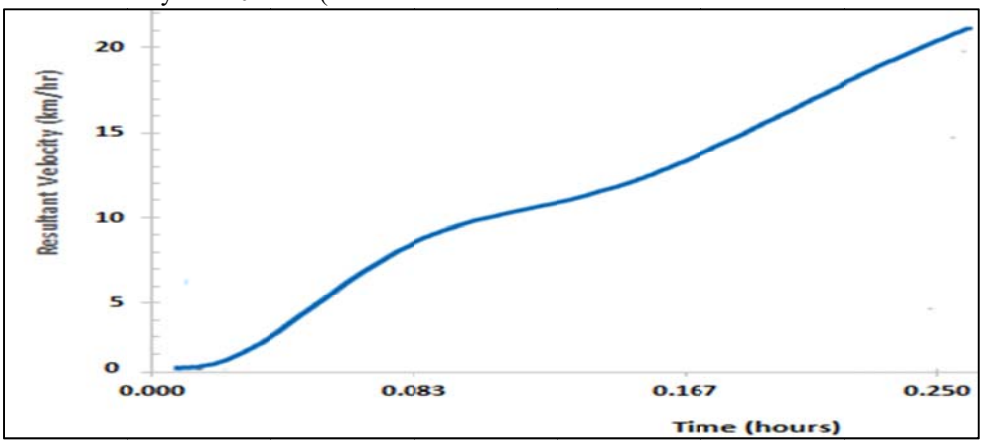

Figure 24; Resultant velocity of the vehicle

3.4 Results on the airspeed of the vehicle :

The airspeed of the vehicle along x and y direction are shown in Figure 25 and Figure 26 respectively. Figure 26; Airspeed impact on the mobility of the vehicle with load along y-direction

The impact of the airspeed on the mobility of the truck with toxic load is displayed in Figure 25 and Figure 26 for x and y direction respectively. The effect of air speed was not stable but normalized after 0.2 hrs (which is 12 minutes). The unstable airspeed affected the mobility of the vehicle by impacting on the speed of the vehicle; slowing down the mobility of the load. The resultant airspeed plot is shown in Figure 27.

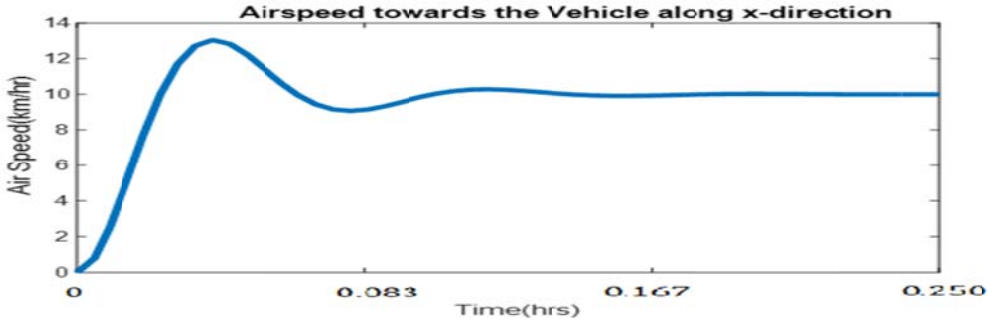

Figure 25; Airspeed impact on the mobility of the vehicle with load along x-direction

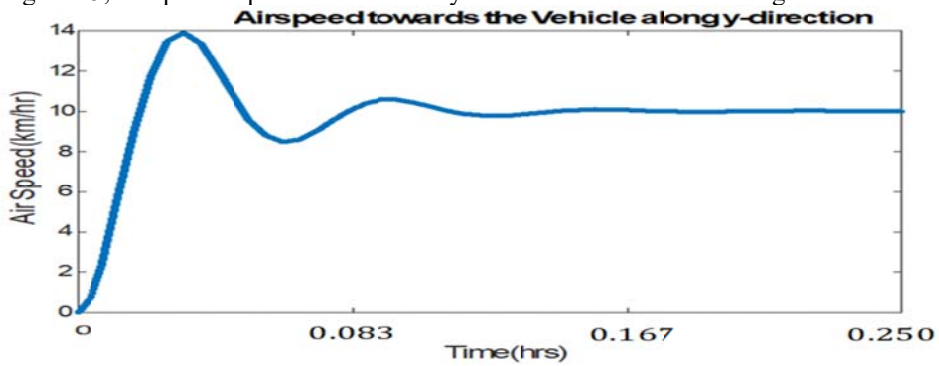

Figure 26; Airspeed impact on the mobility of the vehicle with load along y-direction

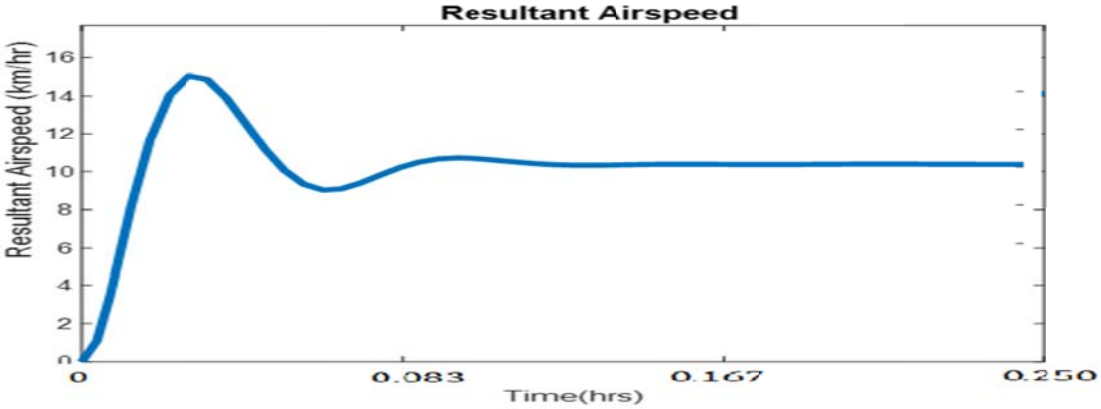

Figure 27; Resultant airspeed impact on the vehicle

3.5 Results on the drag force from the load:

The unstable rise and fall of airspeed affected the mobility of the vehicle due to the toxic waste load. The drag force from the load on the vehicle for y-direction, x-direction and the resultant drag force were shown in Figure 28, Figure 29 and Figure 30 respectively. The drag force in Figures 28, Figure 29 and Figure 30 exhibited the same property of increasing dynamically then stabilized at the 0.2 hour. The increase in the drag force from the container lowers the speed of the vehicle per period and the higher the weight of the load, the more impact it has on the mobility of the vehicle.

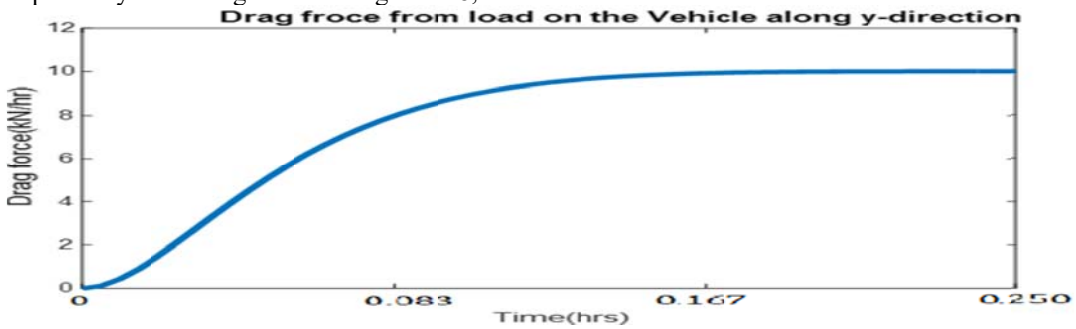

Figure 28; Drag force from the load on the vehicle along y-direction

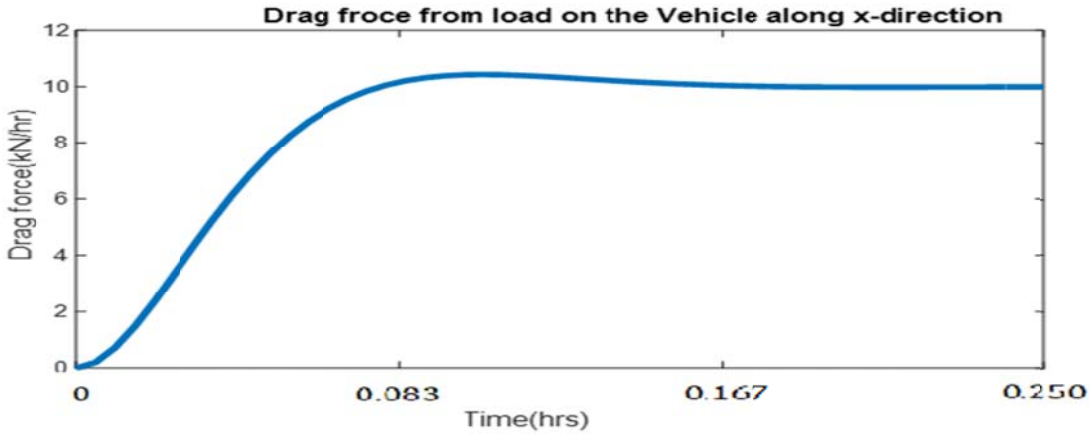

Figure 29; Drag force from the load on the vehicle along x-direction

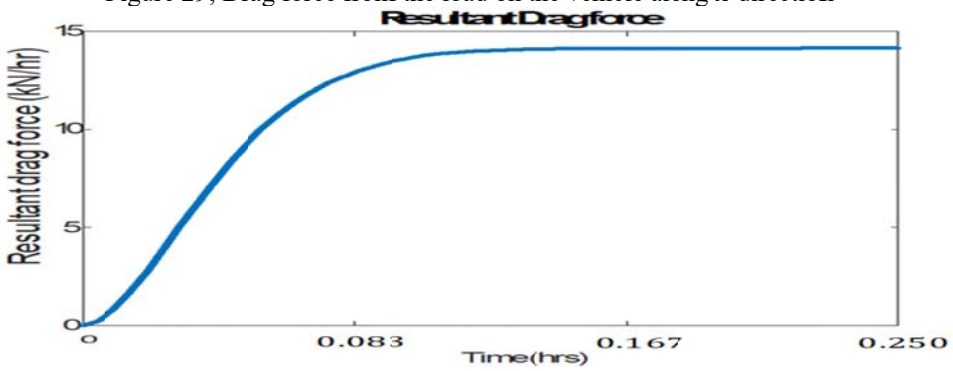

Figure 30; Resultant drag force of the load on the vehicle during motion

3.6 Results on the drag moments on the vehicle from external forces:

The drag moments on the vehicle from external forces for x-direction, y-direction and resultant drag moments is shown in Figure 31, Figure 32 and Figure 33 respectively. The drag moments on the vehicle shown in Figure 31, Figure 32 and Figure 33 increased normally and became saturated after 0.2 hours. The steadiness and stability of drag moments ensures smooth mobility of the vehicular movement. But the higher the drag moments of the external forces exerted on the vehicular movement, the lower the speed of the vehicle.

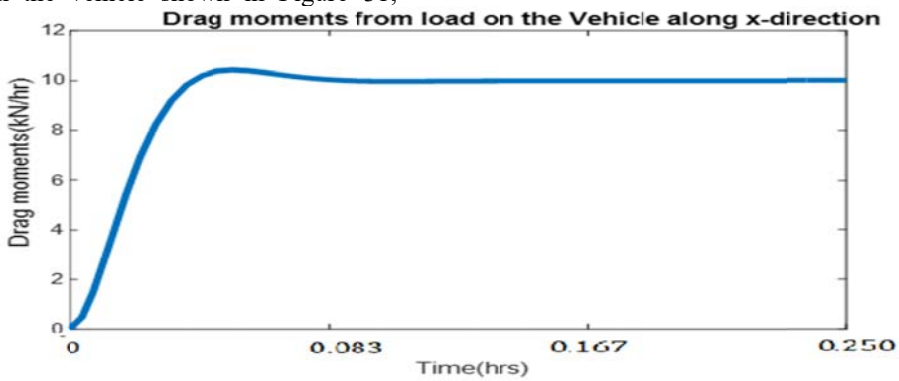

Figure 31; Drag moments from external forces on the vehicle mobility in x-direction

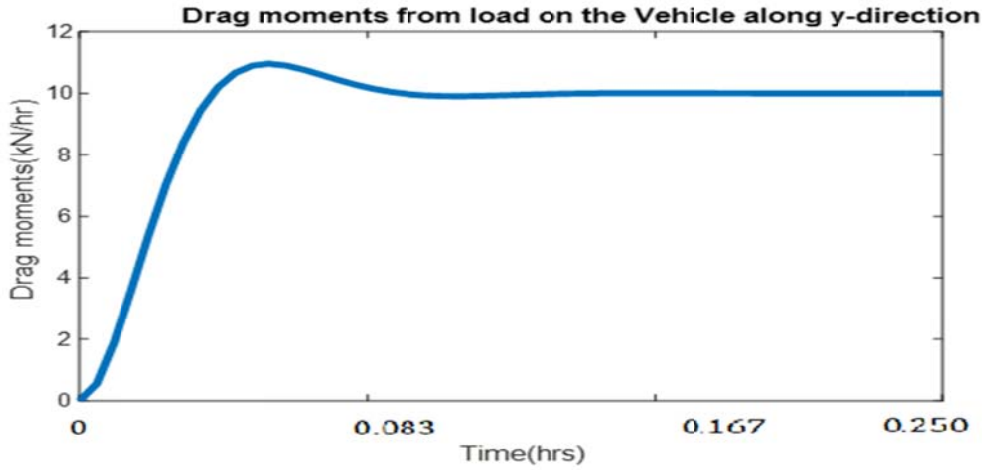

Figure 32; Drag moments from external forces on the vehicle mobility in y-direction

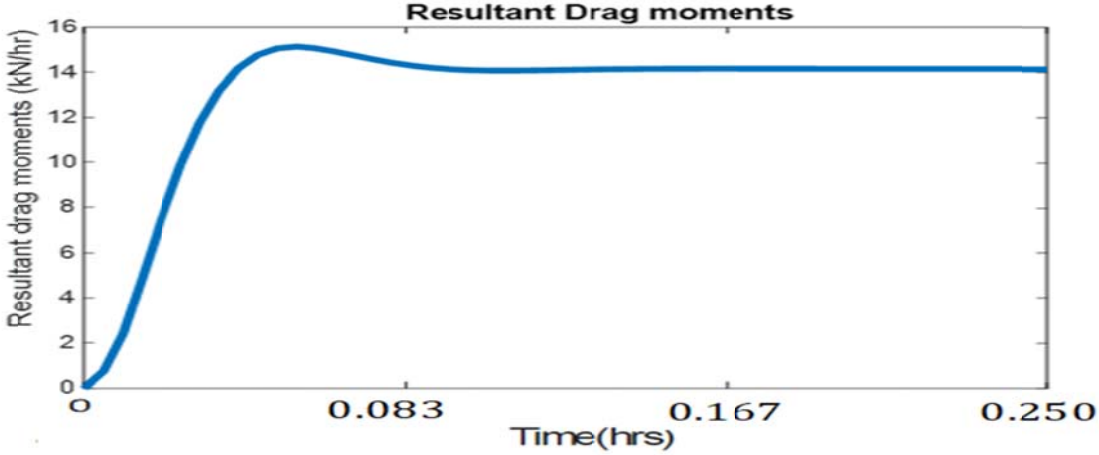

Figure 33; Resultant Drag moments from external forces on the vehicle mobility

3.7 Results on the slip angle of the wheel of the vehicle

The slip angle of the wheel of the vehicle along the x-direction, y-direction and resultant slip angle is shown in Figure 34, Figure 35 and Figure 36. The slip angle of the wheel of the vehicle for x, y directions with the resultant slip showed the prospect of sinusoidal nature and rise and fall as the truck encounters bends and slopes. The higher the slip angle of the wheel, the lower the speed of the vehicle.

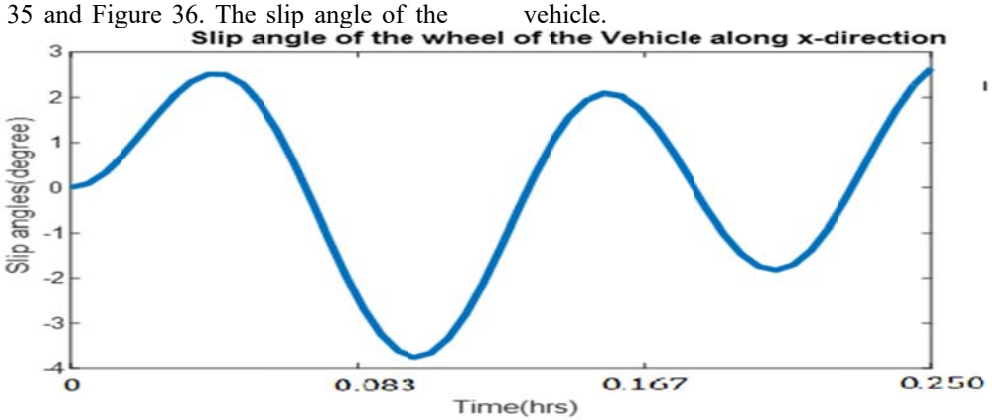

Figure 34 ; Slop angle of the wheel of the vehicle with load along x-direction

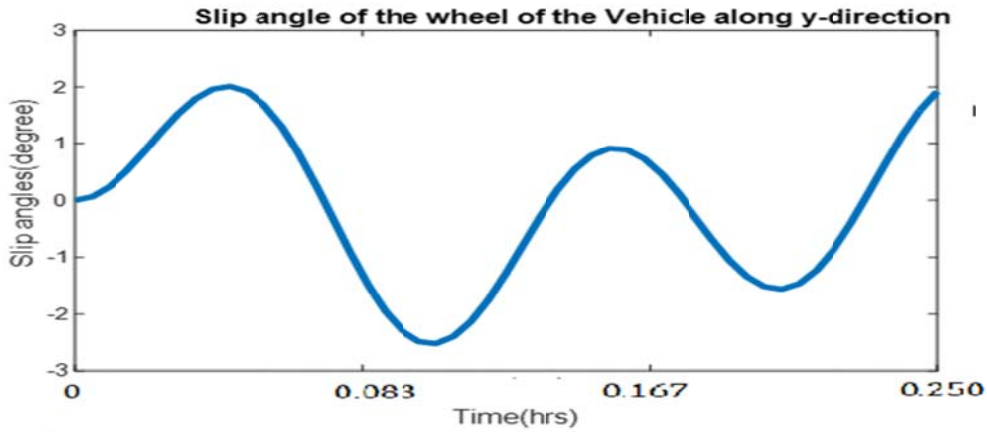

Figure 35; Slip angle of the wheel of the vehicle with load along y-direction

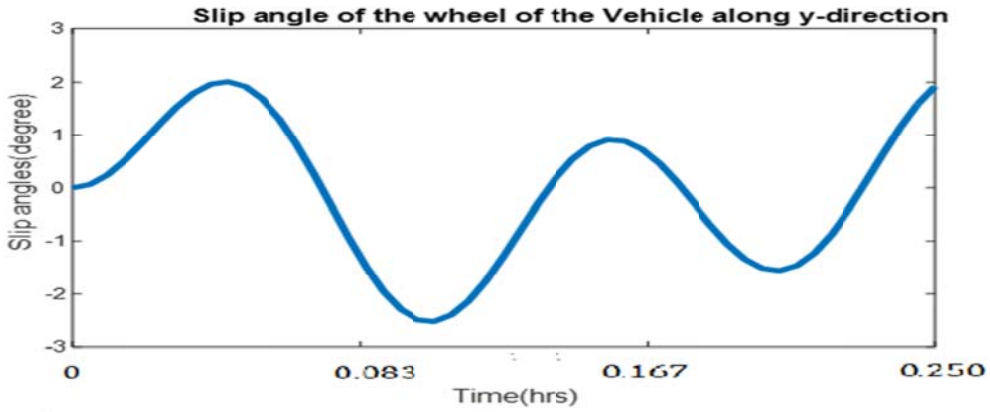

Figure 36; Resultant slip angle of the Vehicle

3.8 Results on the velocity of the vehicle transmitted by the sensors:

The velocity of the vehicle transmitted by the sensors is shown in Figure 37. The same velocity of the vehicle with the toxic load was transmitted by the sensors and it increased progressively and normalized at the 0.2 hour. The constant rise of the velocity was to enable balance with the forces acting on the vehicle so as to achieve a normal velocity as shown in Figure 37.

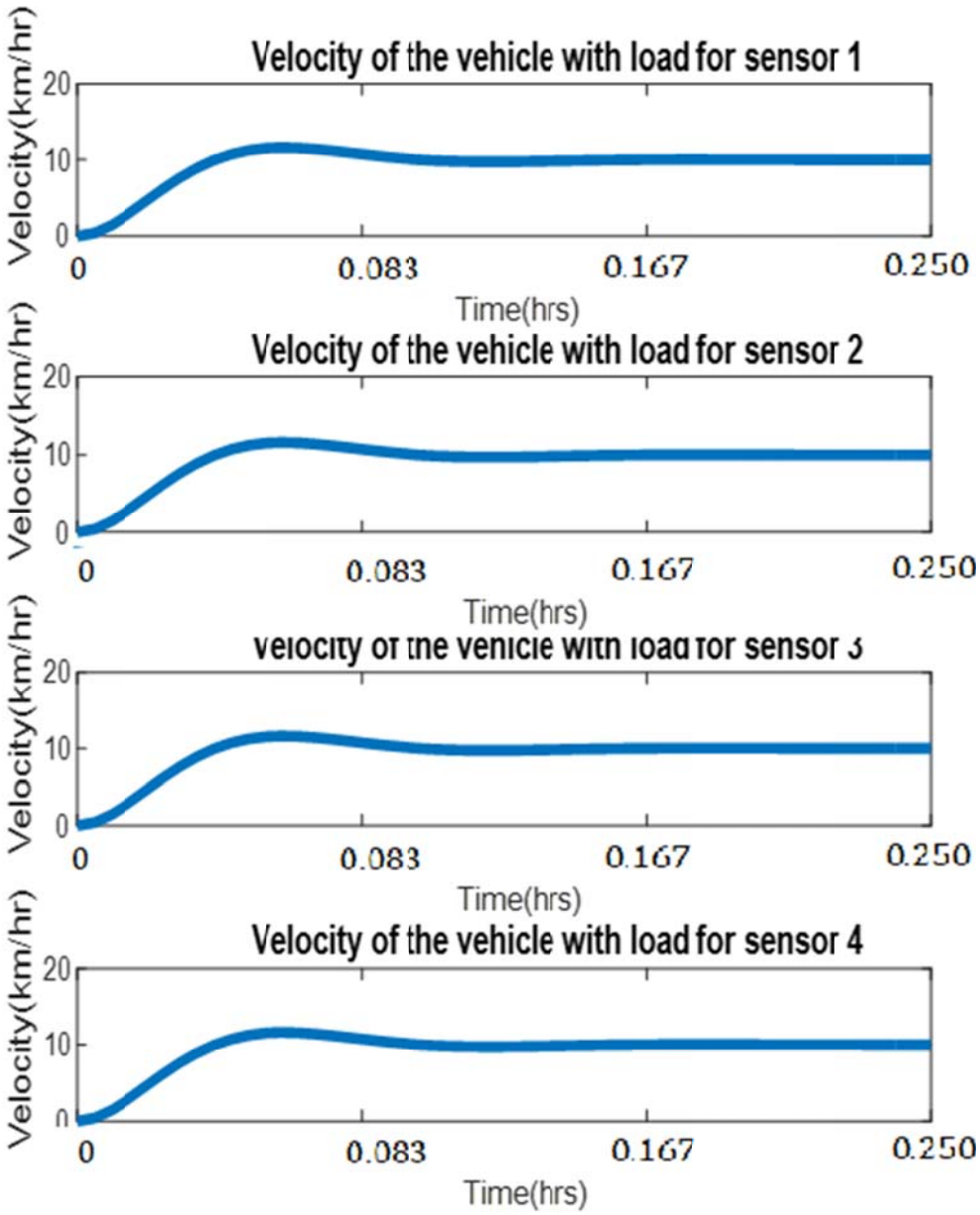

Figure 37; Velocity of the vehicle transmitted by the sensors

3.9 Results on the force exerted on the load:

The force exerted on the load in x-direction, y-direction and the resultant force are shown in Figure 38, Figure 39 and Figure 40 respectively. The resultant force exerted on the load is shown in Figure 38, Figure 39 and Figure 40 for x-direction, y-direction and the resultant force respectively. The higher the force exerted on the load, the lower the speed of the vehicle.

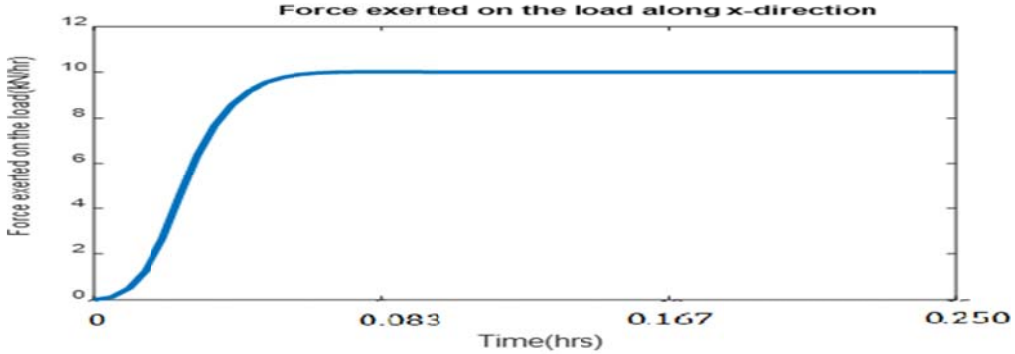

Figure 37; Total force exerted on the load in x-direction

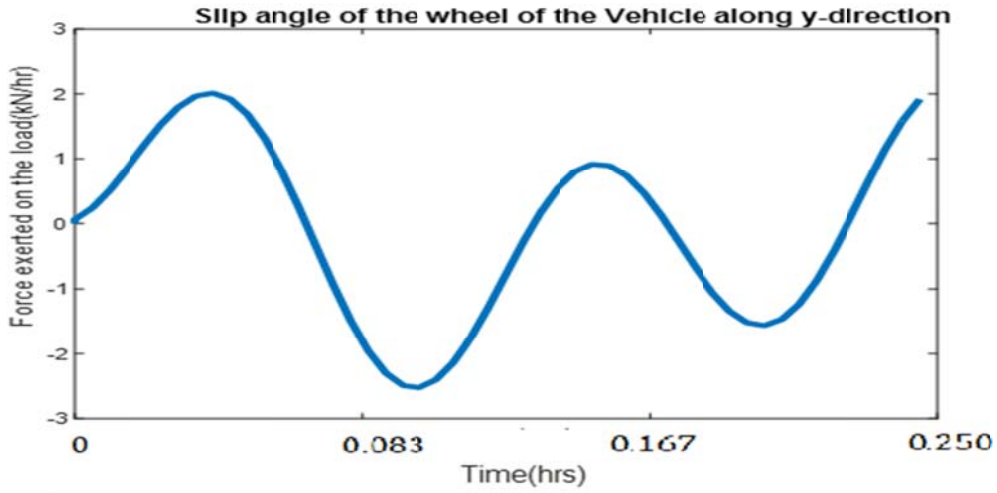

Figure 39; Total force exerted on the load in y-direction

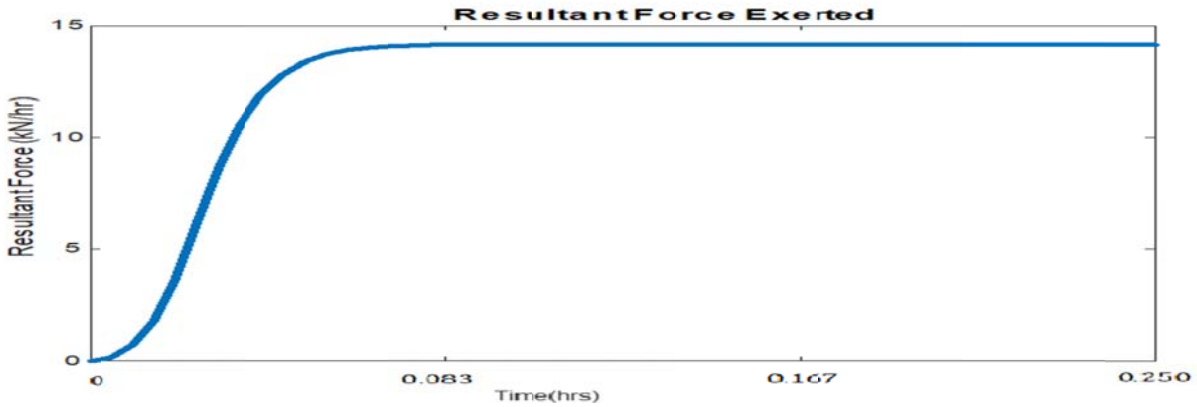

Figure 40; Resultant force exerted

3.10 Results on the weight of the container as transmitted by the sensors:

The weight of the container as transmitted by the sensors during normal condition is shown in Figure 41. The weight of the container reduced during the mobility of the vehicle and normalized at normalized speed. Hence, the weight of the container is affected by the speed variation of the vehicle. The weight of the container at normal condition during deceleration is shown in Figure 42. During deceleration of the truck, it was observed from Figure 42 that the weight of the truck increased as the truck decelerates and the weight was more on the sensors 1 and 2 (the sensors placed at the front of the toxic waste load).

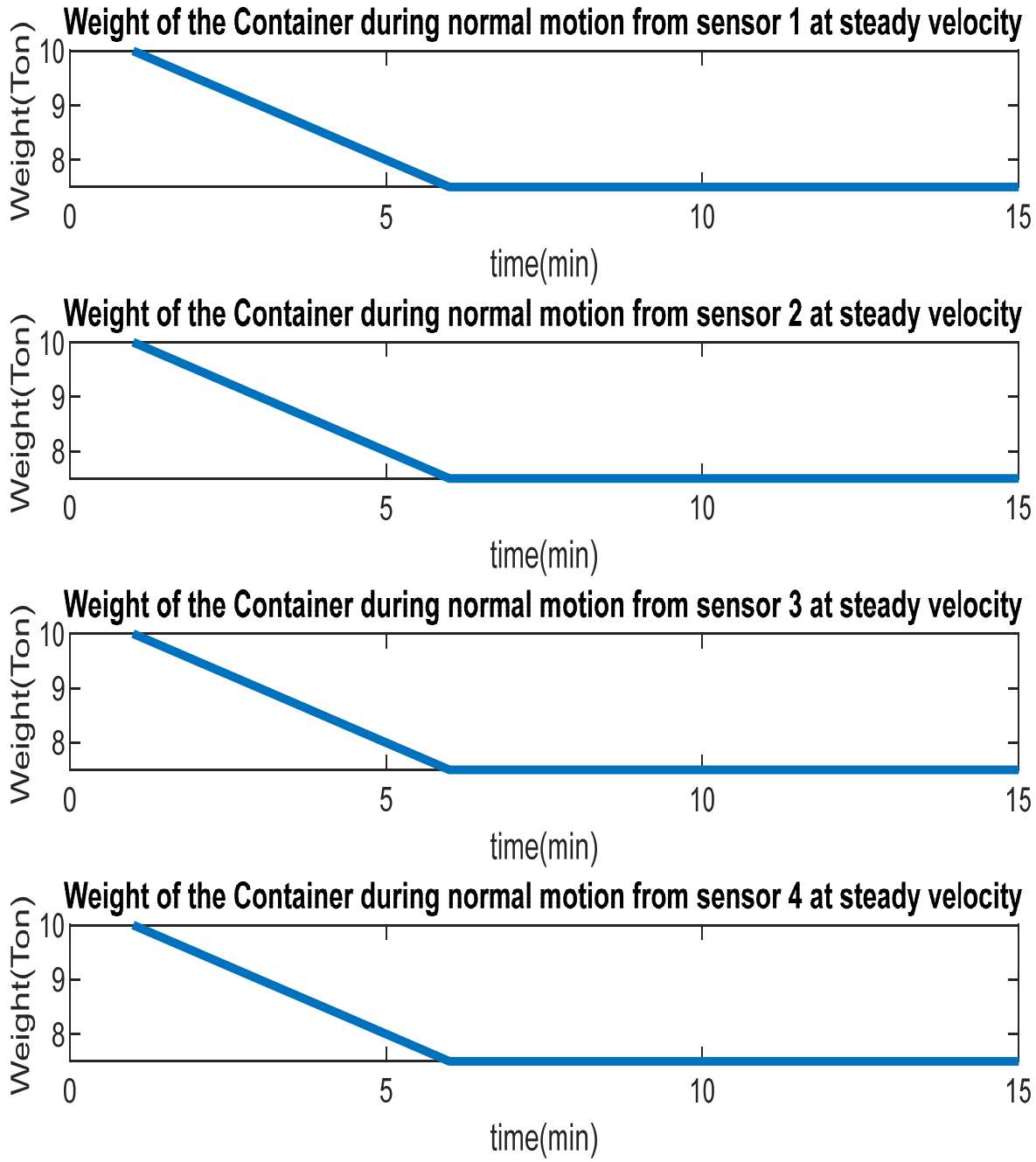

Figure 4.41; Weight of the container at normal condition

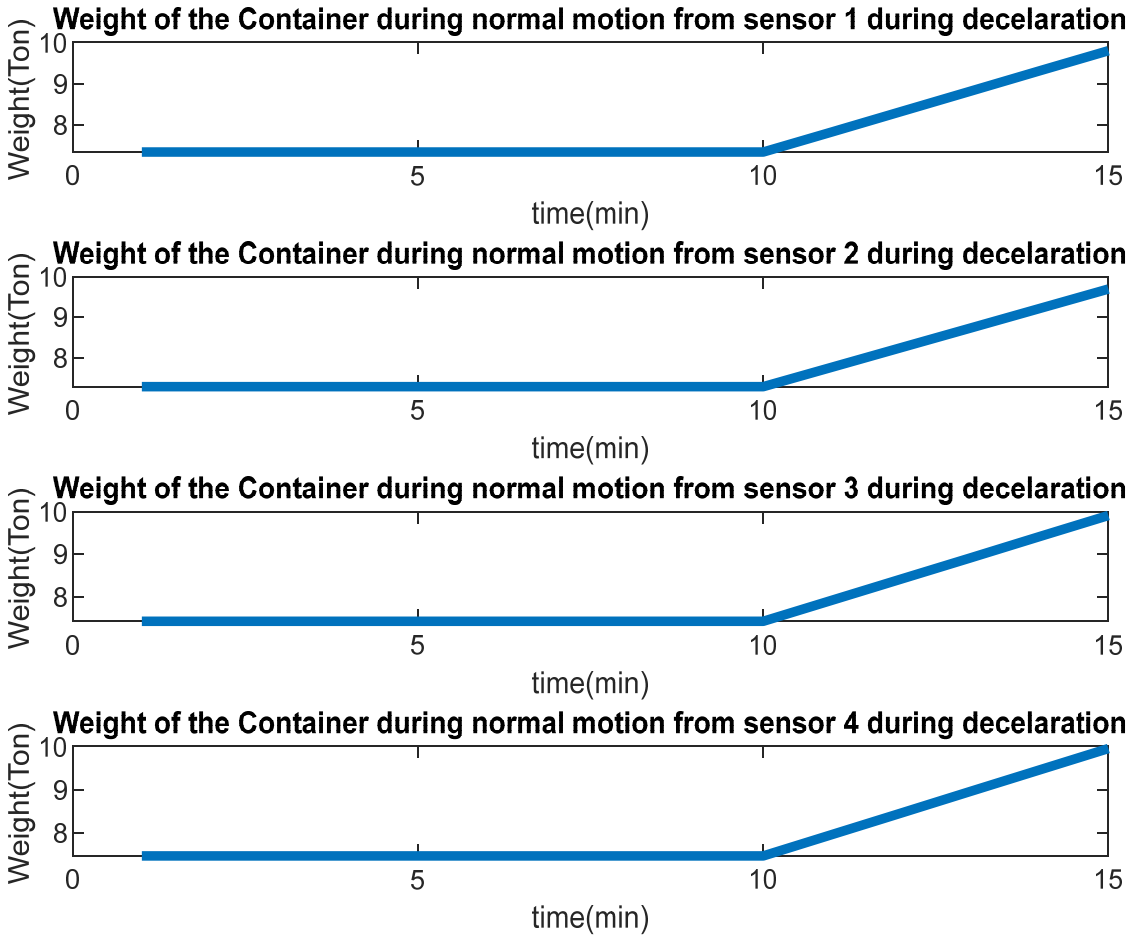

Figure 42; Weight of the toxic container during deceleration of the truck

3.11 Results on the weight of the container at static condition:

The weight of the container at static point (absence of vehicular motion) is shown in Figure 43 (at both velocity and acceleration being zero). The absence of velocity and acceleration implies that the truck with the toxic was not in motion. The load of the waste in the container was 10 tonnes which means for the period of 15mins at static position, the load from all the sensors was 10 tonnes.

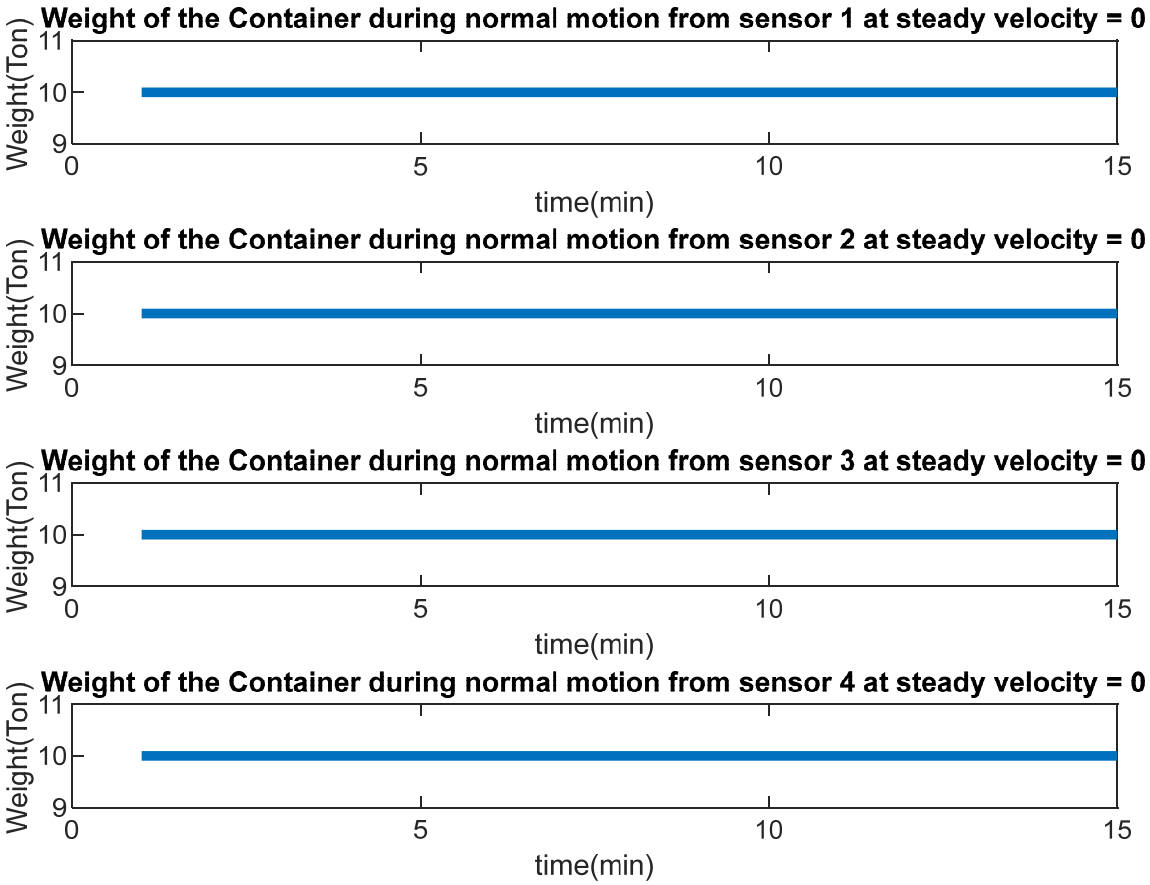

Figure 43; Weight of the container at static velocity

4 CONCLUSION

The study presented analytical approach to characterize the weight and some key motion parameters of a solid waste container as it is being transported to the destination of the waste. The analytical models are essential for determination of the incidences of tempering of the waste while on transit. This particular work focused on the occasion where the vehicle conveying the solid waste container is on normal motion condition; meaning the vehicle is in constant velocity, there is no acceleration, deceleration, and no obstruction and not on a sloppy terrain. Under this condition, the analytical models are used to characterize the weight, air drag, velocity and other resultant parameters that will help automated decision support mechanism to determine when there is likelihood of tampering of the solid waste. These parameters are captured by sensors installed on the solid waste container and sent through a wireless communication channel to a remote computer system for further analysis and actions.

REFERENCES

1. Rahman, M. S., Peeri, N. C., Shrestha, N., Zaki, R., Haque, U., & Ab Hamid, S. H. (2020). Defending against the Novel Coronavirus (COVID-19) outbreak: How can the Internet of Things (IoT) help to save the world?. *Health policy and technology*, *9*(2), 136.
2. Mouha, R. A. R. A. (2021). Internet of things (IoT). *Journal of Data Analysis and Information Processing*, *9*(02), 77.
3. Sosunova, I., & Porras, J. (2022). IoT-enabled smart waste management systems for smart cities: A systematic review. *IEEE Access*, *10*, 73326-73363.
4. Shukla, S., & Hait, S. (2022). Smart waste management practices in smart cities: Current trends and future perspectives. In *Advanced organic waste management* (pp. 407-424). Elsevier.
5. Czekała, W., Drozdowski, J., & Łabiak, P. (2023). Modern technologies for waste management: A review. *Applied Sciences*, *13*(15), 8847.
6. Pardini, K., Rodrigues, J. J., Diallo, O., Das, A. K., de Albuquerque, V. H. C., & Kozlov, S. A. (2020). A smart waste management solution geared towards citizens. *Sensors*, *20*(8), 2380.
7. Ugwuishiwu, B. O., Nwoke, O. A., Okechukwu, C. H., & Echiegu, E. A. (2020). GIS-based system analysis for waste bin location in Enugu municipality. *Agricultural Engineering International: CIGR Journal*, *22*(4), 250-259.
8. Algarni, D. A., & Ali, A. E. (1998). Mapping waste-disposal sites using SPOT remote sensor data: Riyadh case. *Journal of King Saud University-Engineering Sciences*, *10*(1), 15-29.

9. Adedotun, A. A., Sridhar, M. K. C., & Coker, A. O. (2020). Improving municipal solid waste collection system through a GIS based mapping of location specific waste bins in Ibadan Metropolis, Nigeria. *The Journal of Solid Waste Technology and Management*, *46*(3), 360-371.
10. Kashid, S., Ajay, N., & Karbhari, K. (2015). Solid Waste Management: Bin Allocation and Relocation by Using Remote Sensing & Geographic Information System. *International Journal of Research in Engineering and Technology*, *4*(12).
11. Faccio, M., Persona, A., & Zanin, G. (2011). Waste collection multi objective model with real time traceability data. *Waste management*, *31*(12), 2391-2405.
12. Bugge, M. M., Fevolden, A. M., & Klitkou, A. (2019). Governance for system optimization and system change: The case of urban waste. *Research Policy*, *48*(4), 1076-1090.
13. de Souza Melaré, A. V., González, S. M., Faceli, K., & Casadei, V. (2017). Technologies and decision support systems to aid solid-waste management: a systematic review. *Waste management*, *59*, 567-584.
14. Daughton, C. G. (2018). Monitoring wastewater for assessing community health: Sewage Chemical-Information Mining (SCIM). *Science of The Total Environment*, *619*, 748-764.
15. Mmereki, D., Baldwin, A., Hong, L., & Li, B. (2016). The management of hazardous waste in developing countries. *Management of hazardous wastes*, *6*(8), 39-50.